

Convex digital polygons, maximal digital straight segments and convergence of discrete geometric estimators

François de Vieilleville, Jacques-Olivier Lachaud
LaBRI, Univ. Bordeaux 1
351 cours de la Libération, 33405 Talence, France.
`{devieill,lachaud}@labri.fr`

Fabien Feschet
LAIC, Univ. Clermont 1,
IUT, Campus des Cézeaux, 63172 Aubière Cedex, France.
`feschet@laic.u-clermont1.fr`

July 11, 2006

Abstract

Discrete geometric estimators approach geometric quantities on digitized shapes without any knowledge of the continuous shape. A classical yet difficult problem is to show that an estimator asymptotically converges toward the true geometric quantity as the resolution increases. We study here, on Convex Digital Polygons, the convergence of local estimators based on Digital Straight Segment (DSS). This problem is closely linked to the asymptotic growth of maximal DSS, for which we show bounds both about their number and sizes. These results not only give better insights about digitized curves but indicate that curvature estimators based on local DSS recognition are not likely to converge. We indeed invalidate a conjecture which was essential in the only known convergence theorem of a discrete curvature estimator. The proof involves results from arithmetic properties of digital lines, digital convexity, combinatorics, continued fractions and random polytopes.

1 Introduction

Estimating geometric features of shapes or curves solely on their digitization is a classical problem in image analysis and pattern recognition. Some of the geometric features are global to the curve: area, perimeter, moments. Others are local: tangents, normals, curvature. Algorithms that performs this task on digitized objects are called *discrete geometric estimators*. In the following, any algorithm estimating a local geometric quantity within a fixed size neighborhood will be called *local discrete geometric estimator*. We choose to separate them from *local adaptive discrete geometric estimators* whose computation windows

may depend (in size) on the resolution. In this paper we consider the Gauss digitization as the digitization process. An interesting property these estimators should have is to converge towards the continuous geometric measure as the digitization resolution increases. This property is also called *multi-grid convergence* [16]. However, few estimators have been proved to be multi-grid convergent. In all works, shapes are generally supposed to have a smooth boundary (at least twice differentiable) and either to be convex or to have a finite number of inflexion points. The shape perimeter estimation has for instance been tackled in [18]. It proved the convergence of a perimeter estimator based on curve segmentation by maximal DSS. The speed of convergence of several length estimators has also been studied in [5]. Klette and Žunić [17] survey results about the convergence (and the speed of convergence) of several global geometric estimators. They show that discrete moments converge toward continuous moments. As far as we know, only Cœurjolly [4] has initiated works to establish the possible convergence of local adaptive estimators of tangents and curvature. He shows that estimators based on digital straight segment (DSS) recognition may converge if the length of DSS on the digitized curve grows as fast as $O(m^{\frac{1}{2}})$ as the digitization step $\frac{1}{m}$ tends toward 0. Determining the asymptotic growth of DSS along digitized curve is thus crucial for establishing the asymptotic behavior of local adaptive geometric estimators.

This is precisely the objective of this paper, and is achieved with Theorem 5.1. To do so, we relate two notions usually disconnected when studying objects in the digital plane: maximal segments defined on digital curves and edges of convex digital polygons. These notions play complementary roles when estimating geometric parameters on digital objects, when determining its convexity or when observing asymptotic properties of finer and finer shape digitizations.

Maximal segments of a digital curve are DSS not strictly included in any other DSS of the curve. Efficient algorithms have been proposed to extract them and compute their characteristics [8] as well as optimal algorithms to recover the whole set of maximal segments. They are useful when estimating the local geometry of digital curves like tangent direction or curvature [10, 20]. Through them digital curves can be polygonized into the minimum number of straight segments [11]. Maximal segments can be used to decide whether or not a polyomino is convex [22]. As stated above, when observed on object digitizations, the growth rate of their length indicates for some geometric estimators if they converge toward the continuous geometric quantity and at which rate [4].

On the other hand, a *Convex Digital Polygon* (CDP) is a set of lattice points whose convex hull has the same digitization. Its *vertices* are defined as its minimum subset whose convex hull has same digitization, and its *edges* are DSS joining two consecutive vertices. One characterization of digital convexity for a set of lattice points is exactly to be a CDP [15]. Since CDP are digitizations of convex shapes, their asymptotic properties when digitized with finer and finer grid have also been studied. For instance, asymptotic bounds on the number and length of edges have been exhibited for Gauss digitizations of smooth convex shapes [1], and extended to nD in [2]. Interestingly, these bounds are related to random polytopes and have applications in linear integer programming. Along the same lines, other works [17] give tight upper bounds on the number and length of edges for CDPs inscribed in a grid square (a CDP is called *lattice*

convex polygon in this work).

Here we take a specific interest in the maximal segments defined on the boundary of a CDP. Intuitively, these maximal segments should have a close link with the edges of the CDP: the latter are indeed digital straight line segment, but are not generally maximal. However few results can be found in the literature. To our knowledge the only significant results are in [7, 9]: a maximal segment may absorb at most $O(\log m)$ edges for CDP in a $m \times m$ grid square; the length of the *smallest* maximal segment is upper bounded by $O(m^{\frac{1}{3}} \log m)$. This upper bound had consequences on a digital curvature estimator based on circumscribed circle computation [6], which was thought to be multi-grid convergent and whose performances are among the best ones in practice at low resolution. However, as stated above, the proof of the convergence requires that the growth of the maximal segments follow $O(m^{\frac{1}{2}})$ [4]. The conjecture was thus disproved on some points of the curve, although it was still possible that the estimator be convergent on a subset of the curve with non-zero measure.

In this work, we go further in establishing the links between maximal segments and edges of CDP. Most of the new results are obtained by using well known recursive combinatoric representation of a digital straight segment called *pattern*.

We first present the main definitions and used tools in Section 2. The notion of *pattern* is given in Section 2.4. We then establish links between maximal segments and CDP (Section 3). The main results of this section are upper and lower bound on the number of maximal segment. We obtain, in Section 4, the asymptotic upper and lower bounds for the *average* length of maximal segments along a CDP enclosed in a grid of size $m \times m$. We then study the asymptotic of the previous results with respect to increasing m in section 5. We conclude Section 5 by a refutation of the hypothesis used in the previously mentioned curvature estimator convergence proof. We finally present some conclusions and perspectives in Section 6.

2 Definitions and tools

We now precisely detail in this part the main objectives of this paper and introduce the outline of our proof. To begin, we recall the digitization process used in this paper and its associated digital boundary. We pursue with the precise introduction of the Convex Digital Polygon (CDP) followed by the notions of standard lines and digital straight segments. The result of Balog and Bárány [1] is a central tool in our study and we present it as well as a sketch of its use in our proof. All along the paper, when results are announced without proof we always refer to the technical report [9] for full proofs.

2.1 Digitization and digital curve

Let S be a subset of \mathbb{R}^2 , its Gauss digitization is defined as $\mathcal{D}(S) = S \cap \mathbb{Z}^2$. We also define the dilatation of S by a real factor r as $r \cdot S$. The Gauss digitization at resolution m is then defined as: $\mathcal{D}_m(S) = \mathcal{D}(m \cdot S)$. Thus, the considered digitized objects are subsets of \mathbb{Z}^2 . We precise that this digitization is equivalent to intersecting S with $\frac{1}{m}\mathbb{Z} \times \frac{1}{m}\mathbb{Z}$ up to a scale factor.

4-connectedness defines the adjacency relations on digital objects, which means that the neighborhood of a point in the digital plane is composed of its up and down, and left and right neighbors. Among the 4-connected subsets of \mathbb{Z}^2 , we focus on *convex digital polygons* which are also called lattice convex polygons [25].

Definition 2.1. A convex digital polygon (CDP) Γ is a subset of the digital plane with a single 4-connected component equal to the digitization of its convex hull, i.e. $\Gamma = \mathcal{D}(\text{conv}(\Gamma))$. Its vertices $(V_i)_{i=1..e}$ form the minimal subset for which $\Gamma = \mathcal{D}(\text{conv}(V_1, \dots, V_e))$.

The asymptotic study presented later-on in this paper requires the study of Gauss digitizations of convex shapes with \mathcal{C}^3 boundary and positive curvature. We show that for resolutions larger than a threshold which depends on the considered shape, the Gauss digitization for such resolutions always brings a *convex digital polygon*. This rely on two lemmas whom proofs are presented in appendix:

Lemma 2.2. Let S be a convex subset of \mathbb{R}^2 then $\mathcal{D}(S) = \mathcal{D}(\text{conv}(\mathcal{D}(S)))$

Lemma 2.3. For a given S where S is a plane convex body with \mathcal{C}^3 boundary and positive curvature, there exists m_S such that for all $m \geq m_S$, $\mathcal{D}_m(S)$ is 4-connected.

For large enough resolution, the Gauss digitizations of convex shapes with \mathcal{C}^3 boundary and positive curvature have a single 4-connected component and are equal to the digitization of the convex hull of their Gauss digitization, they are thus by definition convex digital polygons.

We can now study the digital boundary of convex digital polygons considering the Grid Cell Model with *2-cells* (see [16] Chap. 2). In this model, each point of a digitized object is considered as a closed square whom side is equal to 1. Its topological border defines a Jordan curve in \mathbb{R}^2 . Considering the intersection of this curve with $(\mathbb{Z} + \frac{1}{2}) \times (\mathbb{Z} + \frac{1}{2})$, we obtain the set of elements constituting the *digital boundary* of our digitized object. This boundary is denoted by C . We number the points of C incrementally as we visit them when moving clock-wise along the topological border of the digitized object. Thus each point on the digital boundary has one predecessor and one successor. The points of the digital boundary are noted (C_k) and a set of successive points ordered increasingly from index i to j will be conveniently denoted by $[C_i C_j]$ when no ambiguities are raised. Those notations are pictured on Fig. 1. Consequently in the following we restrict our study to the geometry of such 4-connected digital path.

2.2 Digital Boundary Of Convex Digital Polygons

We have defined convex digital polygons as particular subsets of \mathbb{Z}^2 and their usual features are defined from those points, namely vertices and edges. We can consider the vertices and edges on the digital boundary of a CDP as if they were on the CDP itself. Interestingly, the number of edges and vertices on a CDP and the number of edges and vertices on its digital boundary only differ by a constant. Indeed, all edges on the CDP whose direction belongs to $]0, \frac{\pi}{2}[$ (when edges are oriented clock-wise) belong to the digital boundary of the CDP when shifted with the vector $(-\frac{1}{2}, \frac{1}{2})$ (see Fig. 2). Other edges are obtained

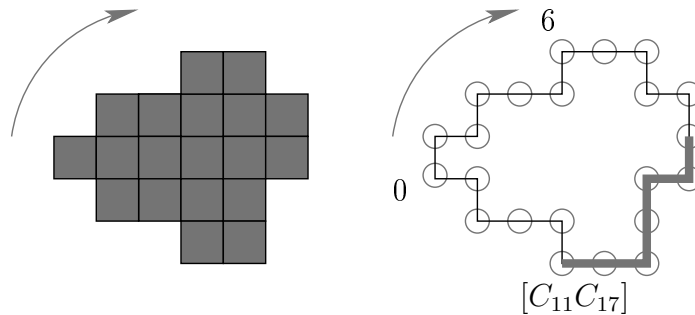


Figure 1: A digitized object considering the Grid Cell Model with 2-cells (left) and its digital boundary C (right).

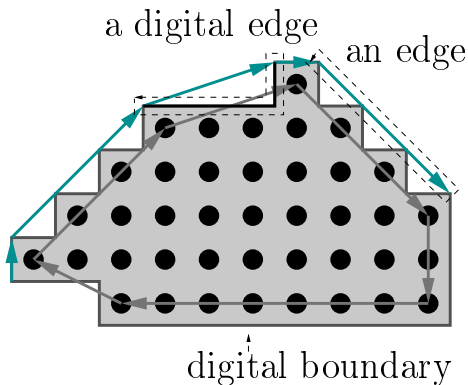


Figure 2: A convex digital polygon, its edges and a digital edge.

symmetrically depending on their direction. As a result, if we denote by $n_e(\Gamma)$ the number of edges on the CDP, its digital boundary has at most $n_e(\Gamma) + 4$ edges and at least $n_e(\Gamma)$.

As we consider asymptotic studies where $n_e(\Gamma)$ increases and tend toward infinity, we denote by $n_e(\Gamma)$ these two quantities. Similarly, we denote the perimeter by $\text{Per}(\Gamma)$.

An *edge* is the Euclidean segment joining two consecutive vertices, and a *digital edge* is the digital shortest 4-connected digital segment joining two consecutive vertices. It is clear that we have as many *edges* as *digital edges* and as vertices.

2.3 Standard line, digital straight segment, maximal segments

Definition 2.4. (Réveillès [23]) *The set of points (x, y) of the digital plane verifying $\mu \leq ax - by < \mu + |a| + |b|$, with a, b and μ integer numbers, is called the standard line with slope a/b and shift μ .*

The *standard lines* are the 4-connected discrete lines. The quantity $ax - by$

is called the *remainder* of the line. The points whose remainder is μ (resp. $\mu + |a| + |b| - 1$) are called upper (resp. lower) leaning points. Finite connected portions of digital lines define *digital straight segment*.

Definition 2.5. *A set of successive points $[C_i C_j]$ of C is a digital straight segment (DSS) iff there exists a standard line $D(a, b, \mu)$ containing them. The predicate “ $[C_i C_j]$ is a DSS” is denoted by $S(i, j)$.*

The principal upper and lower leaning points are defined as those with extremal x values. The first index j , $i \leq j$, such that $S(i, j)$ and $\neg S(i, j + 1)$ is called the *front* of i . The map associating any i to its front is denoted by F . Symmetrically, the first index i such that $S(i, j)$ and $\neg S(i - 1, j)$ is called the *back* of j and the corresponding mapping is denoted by B . Maximal segments are defined as those DSS not strictly included in another DSS.

These relations give the four equivalent characterisations of maximal segments:

Definition 2.6. *Any set of points $[C_i C_j]$ is called a maximal segment iff any of the following equivalent characterizations holds: (1) $S(i, j)$ and $\neg S(i, j + 1)$ and $\neg S(i - 1, j)$, (2) $B(j) = i$ and $F(i) = j$, (3) $\exists k, i = B(k)$ and $j = F(B(k))$, (4) $\exists k', i = B(F(k'))$ and $j = F(k')$.*

As a corollary, any DSS $[C_i C_j]$ (hence any point) belongs to at least one maximal segment. If Γ is a convex digital polygon, We will denote by $n_{MS}(\Gamma)$, the number of maximal segment on its digital boundary.

Most of the results demonstrated here are directly transposable to 8-connected curves since there is a natural bijective transformation between standard and naive digital lines. In the paper, all the reasoning is made in the first octant, but it extends naturally to the whole digital plane.

2.4 Use of Balog and Bárány’s theorem

The original theorem published in [1] deals with the convex hull of Gauss digitizations of plane convex body with C^3 boundary and positive curvature for large resolutions. Using Lemma 2.2 and Lemma 2.3 we complete it with the notion of CDP as follows:

Theorem 2.7. *(Adapted from Balog, Bárány [1]) If S is a plane convex body with C^3 boundary and positive curvature then $\mathcal{D}_m(S)$ is a CDP for a big enough m and its number of edges or vertices asymptotically follows*

$$c_1(S)m^{\frac{2}{3}} \leq n_e(\mathcal{D}_m(S)) \leq c_2(S)m^{\frac{2}{3}}$$

where the constants $c_1(S)$ and $c_2(S)$ depend on extremal bounds of the curvatures along S . Hence for a disc c_1 and c_2 are absolute constants.

Theorem 2.7 is used in the sequel as follows: we build lower and upper bounds of the number of maximal segments built on the boundary of a CDP. The upper bound is given by Theorem 3.11 and depends only on the number of edges of the CDP. The lower bound is given by Theorem 3.15 and relies on both the number of edges and the resolution of the digitization. Both bounds are then used in conjunction with Theorem 2.7 to give asymptotic bounds on the number of maximal segments on the boundary of a CDP, with respect to

the resolution of the digitization grid. For the length of maximal segments, we use the same strategy. Upper bound for the length is given by Proposition 4.3 and depends only on the perimeter of the CDP. The lower bound also depends on the perimeter of the CDP. Since the perimeter can be related to the grid size m , we obtain in Theorem 5.1 the asymptotic law of the average length of maximal segments along the boundary of the CDP. Those bounds both depend on m and the constants appearing in Theorem 2.7.

2.5 Recursive decomposition of DSS

We here recall a few properties about *patterns* composing DSS and their close relations with continued fractions. They constitute a powerful tool to describe discrete lines with rational slopes [3, 13]. W.l.o.g. all definitions and propositions stated below hold for standard lines and DSS with slopes in the first octant (e.g. $\frac{a}{b}$ with $0 \leq a \leq b$). In the first octant, only two Freeman moves are possible:

- 0 : one step to the right,
- 1 : one step up.

Definition 2.8. *Given a standard line (a, b, μ) , we call pattern of characteristics (a, b) the succession of Freeman moves between any two consecutive upper leaning points. The Freeman moves defined between any two consecutive lower leaning points is the previous word read from back to front and is called the reversed pattern.*

A pattern (a, b) embedded anywhere in the digital plane is obviously a DSS (a, b, μ) for some μ . Since a DSS has at least either two upper or two lower leaning points, a DSS (a, b, μ) contains at least one *pattern* or one *reversed pattern* of characteristics (a, b) .

It is important to note that if a digital straight segment of characteristics (a, b, μ) contains δ pattern (a, b) and δ' reversed-pattern (a, b) then it has exactly $\delta + 1$ upper leaning points and $\delta' + 1$ lower leaning points. Moreover, we have $\delta' = \delta \pm 1$. However if a digital straight segment has five leaning point it may be constituted of two patterns and one reversed-pattern or two reversed-patterns and one pattern. As a result the number of leaning points of a digital straight segment cannot precisely describe the number of patterns or reversed-patterns.

Even if the arithmetic approach is a powerful tool for digital straight segment recognition, other approach may reveal useful to get analytic properties. We here recall one of those approaches which is connected to continued fractions.

There exists recursive transformations for computing the *pattern* of a standard line from the *simple continued fraction* of its slope (see [3], [25] Chap. 4 and [16] Chap. 9). We choose to focus on Berstel approach, which better suits our purpose.

A *continued fraction* is an expression of the form:

$$z = 0 + \frac{1}{u_1 + \frac{1}{\dots + \frac{1}{u_n + \dots}}}$$

conveniently denoted $[0, u_1, \dots, u_n, \dots]$. The u_i are called *elements* or *partial coefficient* and the continued fraction formed with the $k + 1$ first *partial coefficient* is said to be a *k-th convergent* of z and is a rational number denoted by z_k . The *depth* of a *k-th convergent* equals k . We conveniently denote p_k the numerator (resp. q_k the denominator) of a *k-th convergent*.

We recall a few more relations regarding the way convergents are related and which will be used later on in this paper:

$$\begin{aligned} \forall k \geq 1 \quad p_k q_{k-1} - p_{k-1} q_k &= (-1)^{k+1} & (1) \\ p_0 = 0 \quad p_{-1} = 1 \quad \forall k \geq 1 \quad p_k &= u_k p_{k-1} + p_{k-2} & (2) \\ q_0 = 1 \quad q_{-1} = 0 \quad \forall k \geq 1 \quad q_k &= u_k q_{k-1} + q_{k-2} & (3) \\ z_0 < z_2 < \dots < z_{2i} < \dots < z < \dots < z_{2i+1} < \dots < z_3 < z_1 & (4) \end{aligned}$$

Continued fractions can be finite or infinite, we focus on the case of rational slopes of lines in the first octant, that is finite continued fractions between 0 and 1. Then for each i , u_i is a strictly positive integer. In order to have a unique writing we consider that the last *partial coefficient* is greater or equal to two; except for slope $1 = [0, 1]$.

Let us now explain how to compute the *pattern* associated with a rational slope z in the first octant.

Consider E a mapping from the set of positive rational number smaller than one onto the Freeman-move's words. As we only consider slopes in the first octant, we only consider horizontal steps (denoted by 0) and vertical steps (denoted by 1).

Let us define this mapping as: $E(z_0) = 0$, $E(z_1) = 0^{u_1}1$ and others values are expressed recursively:

$$E(z_{2i+1}) = E(z_{2i})^{u_{2i+1}} E(z_{2i-1}) \quad (5)$$

$$E(z_{2i}) = E(z_{2i-2}) E(z_{2i-1})^{u_{2i}} \quad (6)$$

It has been shown that this mapping constructs the pattern (a, b) for any rational slope $z = \frac{a}{b}$. Fig. 3 exemplifies the construction of an odd pattern using the mapping E .

The Minkowski \mathcal{L}^1 length of $E(z_k)$ equals $p_k + q_k$ and can be expressed recursively using Eq. (2) and (3).

Eq. (4) specifies that even convergents are approximations by lower values and odd convergents are approximations by upper values. It indeed explains that an even pattern z_{even} and an odd pattern z_{odd} are combined to form a more complex pattern z , the slopes verify $z_{even} < z < z_{odd}$.

There exists other equivalent relations for computing numerators and denominators (see [25] Chap. 4 and [16] Chap. 9) and the *splitting formula* can be used to obtain patterns. However the splitting formula uses two k -th convergents with the same depth, whereas we here use two k -th convergents of consecutive depths.

For convenience reasons we say that a slope has an even (resp. odd) depth when its development in continued fractions has an even (resp. odd) depth.

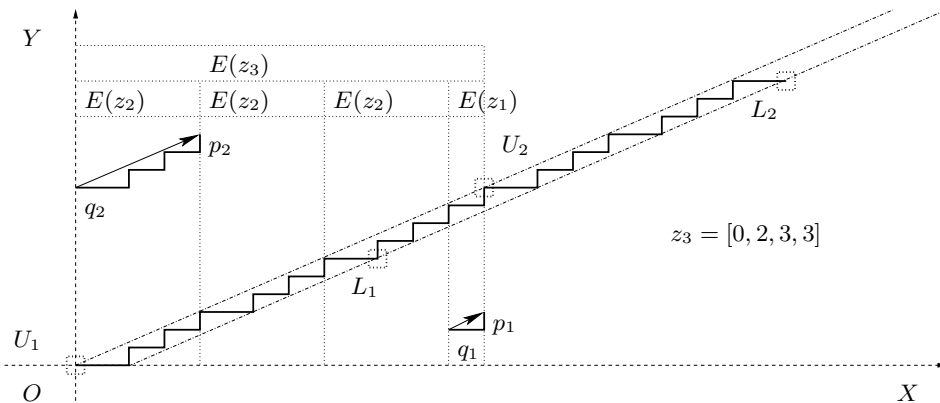


Figure 3: A digital straight segment of characteristics $(10, 23, 0)$ with an odd depth slope, taken between origin and its second lower leaning point.

3 Convex digital polygons and number of maximal digital straight segments

3.1 Introduction

We now study digital straight segments and patterns lying on the digital contour of Convex Digital Polygons (CDP). More precisely, we establish some relations between maximal segments and digital edges of convex shape digitizations.

From characterizations of discrete convexity [15], we obtain the following property.

Proposition 3.1. *Each digital edge of a CDP is either a pattern or a succession of the same pattern whose slope is the one of the edge. In other words, both vertices are upper leaning points of the digital edge.*

Proof. *Points between two successive vertices on the digital curve are always below the real segment linking the two vertices. From [15], $[V_i V_{i+1}]$ is a DSS. Thus the real line linking V_i and V_{i+1} is the upper leaning line of the DSS and both vertices are upper leaning points. \square*

Maximal segments are DSS: between any two upper (resp. lower) leaning points lays at least a lower (resp. upper) leaning point. The slope of a maximal segment is then defined by two consecutive upper and/or lower leaning points. Digital edges are patterns and their vertices are upper leaning points (from Proposition 3.1). Thus, vertices may be upper leaning points but never lower leaning points of maximal segments. Since a digital edge is a DSS, we get:

Lemma 3.2. *A maximal segment cannot be strictly contained into a digital edge.*

Thus, a digital edge is either a maximal segment or a strict subset of a maximal DSS. Since there is one edge associated to one digital edge, the only specific case is when a digital edge is strictly included in a maximal segment. As we have seen, the vertices of a digital edge are upper leaning points of the

digital edge but not necessarily upper leaning points of the maximal segment containing the digital edge. To see what happens on the boundary of the CDP, we notice that a maximal segment is defined by at least three leaning points. They are two cases: ULU corresponding to two upper and one lower leaning points and LUL corresponding to two lower and one upper leaning points. If a maximal segment contains strictly more than three leaning points, it has at least two upper leaning points and we say that it verifies the ULU case also. In the sequel, we study those two cases by relating them respectively to edges and vertices of the CDP. Thanks to these associations, we could describe in Theorem 3.11 an upper bound on the number of maximal DSS.

3.2 Case study

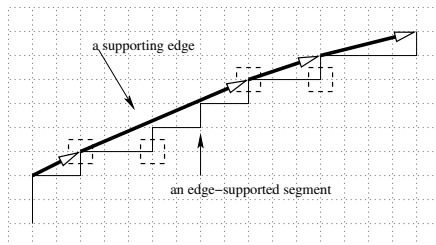


Figure 4: Supporting edge and edge-supported segments of a CDP

We first study the ULU case. Doerksen and Debled [22] proved that principal upper leaning points of maximal segment are vertices of the CDP. Hence, any maximal segment in the ULU case defines a digital edge which links these upper leaning points. This motivates the following definitions (see Fig. 4) and lemma.

Definition 3.3. We call supporting edge, a digital edge whose two vertices define leftmost and rightmost upper leaning points of some maximal segment.

Definition 3.4. We call edge-supported segment, a maximal segment defined by a supporting edge.

Lemma 3.5. A supporting edge defines only one maximal segment: it is the only one containing the edge and it has the same slope. If a maximal segment contains two or more upper leaning points then there is a supporting edge linking its leftmost and rightmost upper leaning points with the same slope. If a maximal segment contains three or more lower leaning points then it contains a supporting edge with the same slope.

Hence, we can associate to any maximal segment in the ULU case its corresponding digital edge. Thus, there is a natural correspondence between ULU maximal segments and a subset of the edges of the CDP.

We then study the LUL case. The only upper leaning point of such a maximal segment is clearly a vertex of the CDP. We thus introduce the following definition (see Fig. 5).

Definition 3.6. We call vertex-supported segment, a maximal segment whose slope is only defined by its two consecutive lower leaning points. Such a segment has only one upper leaning point.

We now relate the number of vertex-supported segments to the number of digital edges.

Proposition 3.9. *On a vertex of the CDP there is at most one vertex-supported segment with an even depth.*

Proof. *The proof is made by contradiction. Consider there exists two vertex-supported segments of even depth. Say MS of depth z_{2i} with L_1, L_2 its lower leaning points (leftmost and rightmost) and U_2 as upper leaning point; MS' of depth z'_{2j} with L'_1, L'_2 its lower leaning points and U_2 as upper leaning point (they share the same vertex as upper leaning point). If $L_1 = L'_1$, then MS and MS' coincide since they are maximal segments (using Lemma 3.7). Consider now that $L'_1 < L_1$, that is the leftmost lower leaning point of MS' lays before the one of MS on the convex discrete curve. In this case it is clear that $[L_1U_2] \subset [L'_1U_2]$. Thus $[L'_1U_2] = l'[L_1U_2]$ with l' some left strict factor of $[L'_1U_2]$. From Proposition B.2 $[L_1U_2]$ has $E(z_{2i-1})^{u_{2i-1}}$ as a right factor. We can now write $[L'_1U_2] = l'lE(z_{2i-1})^{u_{2i-1}}$ with l some left strict factor of $[L_1U_2]$, and $[L'_1U_2]$ contains the pattern $E(z_{2i-1})$. Since $[L'_1U_2]$ is a right subpart of the pattern $E(z'_{2j})$, $E(z_{2i-1})$ is a right strict factor of $E(z'_{2j})$.*

If $z_{2i} = [0, u_1, \dots, u_{2i-1}, u_{2i}]$, from Proposition B.3 the slope z'_{2j} has z_{2i-2} as a $2i - 2$ convergent, and $u'_{2i-1} \geq u_{2i-1}$. Thus $z'_{2j} = [0, u_1, \dots, u_{2i-2}, u'_{2i-1}, u'_{2i}, \dots, u'_{2j}]$. From Proposition B.2 (switching U_1L_1 with U_2L_2 in the proposition) we have $\mathcal{L}^1(\mathbf{U}_2\mathbf{L}_2) = q_{2i-1} + p_{2i-1} = u_{2i-1}(q_{2i-2} + p_{2i-2}) + q_{2i-3} + p_{2i-3}$ and $\mathcal{L}^1(\mathbf{U}_2\mathbf{L}'_2) = q'_{2j-1} + p'_{2j-1}$.

From the writing of $\mathcal{L}^1(\mathbf{U}_2\mathbf{L}'_2)$ and with $u'_{2i-1} \geq u_{2i-1}$, we have $\mathcal{L}^1(\mathbf{U}_2\mathbf{L}'_2) \geq \mathcal{L}^1(\mathbf{U}_2\mathbf{L}_2)$. As a result we have : $L'_1 < L_1 < U_2 < L_2 \leq L'_2$. Using Lemma 3.8 we get a contradiction. \square

Similarly, we obtain the same result for a segment with an odd depth.

Proposition 3.10. *On a vertex of the CDP there is at most one vertex-supported segment with an odd depth.*

We have seen that any edge-supported segment is associated to one edge of the CDP and that to each vertex of the CDP at most two vertex-supported segments can be associated. This leads to the following upper bound.

Theorem 3.11. *If Γ is a CDP, its number of maximal segments is upper bounded by three times its number of edges.*

Proof. *Let us consider the following numbers of maximal segments:*

- n_{ULU} are the edge-supported segments whose slope is given by their upper leaning point. Each of them is linked to a supporting edge.
- n_{LUL}^{even} are the vertex-supported segments with an even depth.
- n_{LUL}^{odd} are the vertex-supported segments with an odd depth.

It is clear that $n_{MS}(\Gamma) = n_{ULU} + n_{LUL}^{odd} + n_{LUL}^{even}$. Moreover we have:

- $n_{ULU} \leq n_e(\Gamma)$.
- $n_{LUL}^{even} \leq n_e(\Gamma)$ from Proposition 3.9.
- $n_{LUL}^{odd} \leq n_e(\Gamma)$ from Proposition 3.10.

Consequently: $n_{MS} \leq 3n_e(\Gamma)$ \square .

3.4 Absorption of digital edges by maximal segments and lower bound

In the previous subsection, we provide an upper bound on the number of maximal segments. The lower bound however depends on the resolution m of the digitization process and will be studied later on. In this subsection, we study the absorption phenomena of digital edges by maximal segments.

We recall that each digital edge of the CDP is a pattern. We now try to find how many edges can be absorbed by a single maximal segment. This is done in three steps. We begin with Lemma 3.12 which examines under which conditions a pattern could be extended by successive patterns so that the resulting set is not a pattern but still a digital straight segment. We then determine how many edges (i.e. patterns) can fit into a maximal segment, first into edge-supported segments and secondly into vertex-supported segments (Theorem 3.13). These results, combined together, give the lower bound for the number of maximal segments wrt the number of edges, which is shown to be log-dependent on the maximal slope depth of digital edges.

Lemma 3.12. *We call P_n a pattern of depth n whose Freeman code is $E(z_n)$. One can build strict right and left factors (called respectively R and L) of P_n such that:*

- (i) $[RP_n]$, $[P_nL]$ and $[RP_nL]$ are DSS of slope z_n ,
- (ii) R and L are patterns (or successions of the same pattern) ,
- (iii) RP_n , P_nL and RP_nL are not patterns,
- (iv) the slope of R is greater than that of P_n and the slope of P_n is greater than that of L ,
- (v) maximal depth of slope of R and L depends on parity of n :

Depth of P_n	maximal depth of R	maximal depth of L
$2i + 1$	$2i + 1$	$2i$
$2i$	$2i - 1$	$2i$

their Freeman moves are such that:

Freeman moves of P_n	Freeman moves of R	Freeman moves of L
$E(z_{2i+1})$	$E(z_{2i})^{u_{2i+1}-r} E(z_{2i-1})$	$E(z_{2i})^{u_{2i+1}-l}$
$E(z_{2i})$	$E(z_{2i-1})^{u_{2i}-r}$	$E(z_{2i-2})E(z_{2i-1})^{u_{2i}-l}$

- (vi) Depth of factors obtained by subtracting R or L from P_n depends on parity of n :

Depth of P_n	depth of $P_n \setminus R$	depth of $P_n \setminus L$
$2i + 1$	$2i$	$2i + 1$
$2i$	$2i$	$2i - 1$

their Freeman moves are such that:

Freeman moves of P_n	Freeman moves of $P_n \setminus R$	Freeman moves of $P_n \setminus L$
$E(z_{2i+1})$	$E(z_{2i})^r$	$E(z_{2i})^l E(z_{2i-1})$
$E(z_{2i})$	$E(z_{2i-2})E(z_{2i-1})^r$	$E(z_{2i-1})^l$

Proof. Since R and L are strict factors of P_n , their Freeman moves are compatible with those of $E(z_n)$, giving same slope when R, P_n and L are put together. Thus $[RP_n]$, $[P_nL]$ and $[RP_nL]$ are DSS of slope z_n . This concludes (i). From

digital straightness we clearly have digital convexity (see [15]). Upper leaning points of this DSS are located at extremities of P_n .

We simply choose among strict factors R and L those that are patterns so that they fit descriptions given in Eq. (5) and Eq. (6). Which brings (ii).

We may now describe them given the parity of n . Consider the case where n is odd (say $n = 2i + 1$), from Eq. (5) we get: $R = E(z_{2i})^{u_{2i+1}-r} E(z_{2i-1})$ and $L = E(z_{2i})^{u_{2i+1}-l}$ with $r > 0$ and $l > 0$. If R and L are longer patterns, they are not anymore strict factors of P_{2i+1} . We see that R is a pattern of depth $2i + 1$ and that L is a succession of the pattern $E(z_{2i})$, with a depth of $2i$. This brings (v) in the odd case.

The slope of R equals $z'_{2i+1} = [0, u_1, \dots, u_{2i}, u_{2i+1}-r] = \frac{p'_{2i+1}}{q_{2i+1}}$. From Eq. (2)

and Eq. (3) we get that $\frac{p_{2i+1}}{q_{2i+1}} = \frac{p'_{2i+1} + r p_{2i}}{q_{2i+1} + r q_{2i}}$. The sign of $z'_{2i+1} - z_{2i+1}$ is that of $p'_{2i+1} q_{2i} - q'_{2i+1} p_{2i}$, and is positive (see Eq. (1)). Thus the slope of R is greater than that of P_{2i+1} . Same reasoning applied to $z_{2i+1} - z_{2i}$ brings that the slope of P_{2i+1} is greater than that of L . Thus (iv) holds in the odd case.

Consider now that n is even (say $n = 2i$), from Eq. (6) we get: $R = E(z_{2i-1})^{u_{2i}-r}$ and $L = E(z_{2i-2}) E(z_{2i-1})^{u_{2i}-l}$. If R and L are longer patterns, they are not anymore strict factors of P_{2i} . Clearly, R has a depth of $2i - 1$ and that of L equals $2i$. This brings (v) in the even case.

The slope of L equals $z'_{2i} = [0, u_1, \dots, u_{2i-1}, u_{2i}-l] = \frac{p'_{2i}}{q_{2i}}$. From Eq. (2) and

Eq. (3) we get that $\frac{p_{2i}}{q_{2i}} = \frac{p'_{2i} + l p_{2i-1}}{q_{2i} + l q_{2i-1}}$. The sign of $z_{2i} - z'_{2i}$ is that of $q'_{2i} p_{2i-1} - p'_{2i} q_{2i-1}$, and is positive (see Eq. (1)). Thus the slope of P_n is greater than that of L . Same reasoning applied to $z_{2i-1} - z_{2i}$ brings that the slope of R is greater than that of P_n . Thus (iv) holds in the even case.

From Eq. (6) and Eq. (5) and preceding results it is clear that RP_n , $P_n L$ and $RP_n L$ cannot be described as patterns which brings (iii).

If n is odd then the factor obtained by subtracting R from P_{2i+1} equals $E(z_{2i})^r$ and subtracting L from P_{2i+1} gives $E(z_{2i})^l E(z_{2i-1})$. In the even case the factor obtained by subtracting R from P_{2i} equals $E(z_{2i-2}) E(z_{2i-1})^r$ and subtracting L from P_{2i} gives $E(z_{2i-1})^l$. Thus (vi) holds. \square

Theorem 3.13 shows that the maximal number of digital edges that may be contained in a maximal segment linearly depends on the depth of its slope.

Theorem 3.13. *We have the following:*

1. *Let E be a supporting edge whose slope has a depth n , $n \geq 2$, then the edge-supported maximal segment associated with E includes at most n other edges on each side of E .*
2. *Any vertex-supported maximal segment whose slope has a depth n includes at most $2n$ edges.*

Proof. *We only provide the proof of the first result and refer to [9] for a similar proof of the second result.*

We construct $2n$ digital edges around E :

- $(R_i)_{1 \leq i \leq n}$ at left of E ,
- $(L_i)_{1 \leq i \leq n}$ at right of E .

These edges are such that $[R_n \dots R_i \dots R_1 E L_1 \dots L_j \dots L_n]$ is a DSS of slope $z_n = a/b$ and has no other upper leaning points but those located on E . E may contain several times the pattern $E(z_n)$. It is clear that $R_n \dots R_i \dots R_1$ (resp. $L_1 \dots L_j \dots L_n$) has to be a right (resp. left) strict factor of $E(z_n)$ to be compatible with it. Moreover R_i is a right strict factor of $E(z_n) \setminus R_{i-1} \dots R_1$ and L_i is a left strict factor of $E(z_n) \setminus L_1 \dots L_{i-1}$. From Proposition 3.1 if $(R_i)_{1 \leq i \leq n}$ and $(L_i)_{1 \leq i \leq n}$ are patterns or successions of the same pattern, then they are digital edges. From Eq. (5) and Eq. (6) two successive digital edges with same depth (say n) cannot form a right or left strict factor of a pattern with same depth. Thus depths of $(R_i)_{1 \leq i \leq n}$ and $(L_i)_{1 \leq i \leq n}$ are decreasing when i increases. Moreover to fulfill convexity properties, slopes of edges are decreasing from R_n to L_n .

We now build $(R_i)_{1 \leq i \leq n}$ when n is odd (say $n = 2i+1$). From Lemma 3.12 (v), R_1 has a depth that equals $2i+1$ and R_2 is a right strict factor of $E(z_n) \setminus R_1$ which is by Lemma 3.12 (vi) a pattern of depth $2i$. Applying again Lemma 3.12(v) brings R_2 with a depth of $2i-1$. Since complexities are decreasing, we only take into account the right part of $E(z_n) \setminus R_1 R_2$ which has a depth equaling at most $2i-1$, that is $E(z_{2i-1})^{r_2}$. We can now build R_3 and R_4 using Lemma 3.12 on $E(z_{2i-1})$. Applying the same reasoning recursively brings other edges as shown on Table 1. Lemma 3.12(iv) also implies decreasing slopes, that is digital convexity.

Constructions for the three other cases are given in Tables 1 and 2 and follow the same reasoning. To satisfy full decomposition each $(u_k)_{1 \leq k \leq n}$ has to be equal or greater than 2. If this condition is not met for some k , than steps associated with it (e.g. any factors containing $u_k - r_j$ or $u_k - l_j$ as powers of some pattern) are skipped. This concludes the proof. \square

The following corollary is based on the proof of Theorem 3.13 by taking the worst-case construction. A similar result related to linear integer programming is in [24]. It may also be obtained by viewing standard lines as intersection of two knapsack polytopes [14].

Corollary 3.14. *The shortest pattern of a supporting edge for which its maximal segment may contain $2n+1$ digital edge is $z_n = [0, 2, \dots, 2]$. If the DCP is enclosed in a $m \times m$ grid, then the maximal number n of digital edges included in one maximal segment is upper bounded as:*

$$n \leq \frac{\log(2\sqrt{2}m)}{\log(1+\sqrt{2})} - 1$$

Proof. From Theorem 3.13 we know that maximal segments may contain at most $2n+1$ digital edges. We further know that these ones are edge-supported segments. We now look for the shortest pattern. To fulfill all conditions, if $z_n = [0, u_1, \dots, u_n]$ is the slope of the pattern then each $u_i, 1 \leq i \leq n$, has to be greater or equal than two. The length of each pattern z_n (say $\mathcal{L}^1(E(z_n))$) can be computed using Eq (2) and (3) and can be expressed as a functional of u_1, \dots, u_n . A closer look these equations brings that: $\frac{\partial \mathcal{L}^1(E(z_n))}{\partial u_i} \geq 0$ for each $1 \leq i \leq n$. As a result, the shortest pattern that matches Theorem 3.13 is such that: $1 \leq i \leq n \quad u_i = 2$ and $u_0 = 0$.

Asymptotically, we get the number $L = [0, 2, \dots, 2, \dots]$, which is a quadratic number equal to $-1 + \sqrt{2}$. Its recursive characterization is $U_n = 2U_{n-1} + U_{n-2}$

Table 1: Constructions of $(R_i)_{1 \leq i \leq n}$ and $(L_i)_{1 \leq i \leq n}$ given n odd.
Constructions of $(R_i)_{1 \leq i \leq n}$ when $n = 2i + 1$

Factor	Freeman moves	Depth
R_1	$E(z_{2i})^{u_{2i+1}-r_1} E(z_{2i-1})$	$2i + 1$
R_2	$E(z_{2i-1})^{u_{2i}-r_2}$	$2i - 1$
R_3	$E(z_{2i-2})^{u_{2i-1}-r_3} E(z_{2i-3})$	$2i - 1$
R_4	$E(z_{2i-3})^{u_{2i-2}-r_4}$	$2i - 3$
\vdots	\vdots	\vdots
R_{2j}	$E(z_{2i+1-2j})^{u_{2i+2-2j}-r_{2j}}$	$2i + 1 - 2j$
R_{2j+1}	$E(z_{2i-2j})^{u_{2i+1-2j}-r_{2j+1}} E(z_{2i-1-2j})$	$2i + 1 - 2j$
\vdots	\vdots	\vdots
R_{2i+1}	$0^{u_1-r_{2i+1}} 1$	1

Constructions of $(L_i)_{1 \leq i \leq n}$ when $n = 2i + 1$

Factor	Freeman moves	Depth
L_1	$E(z_{2i})^{u_{2i+1}-l_1}$	$2i$
L_2	$E(z_{2i-2}) E(z_{2i-1})^{u_{2i}-l_2}$	$2i$
L_3	$E(z_{2i-2})^{u_{2i-1}-l_3}$	$2i - 2$
L_4	$E(z_{2i-4}) E(z_{2i-3})^{u_{2i-2}-l_4}$	$2i - 2$
\vdots	\vdots	\vdots
L_{2j}	$E(z_{2i-2j}) E(z_{2i+1-2j})^{u_{2i+2-2j}-l_{2j}}$	$2i + 2 - 2j$
L_{2j+1}	$E(z_{2i-2j})^{u_{2i+1-2j}-l_{2j+1}}$	$2i - 2j$
\vdots	\vdots	\vdots
L_{2i+1}	$0^{u_1-l_{2i+1}}$	0

with $U_0 = 0$ and $U_1 = 1$. We also have $z_n = [0, \underbrace{2, \dots, 2}_{n \text{ times}}] = \frac{U_n}{U_{n+1}}$.

Solving it leads to $U_n = \frac{\sqrt{2}}{4} ((1 + \sqrt{2})^n - (1 - \sqrt{2})^n)$. Hence asymptotically, $U_n \approx \frac{\sqrt{2}}{4} (1 + \sqrt{2})^n$ and $\lim_{n \rightarrow \infty} \frac{U_n}{U_{n+1}} = L$.

Recall that z_n is the n -th convergent of L . We have $\mathcal{L}^1(E(z_n)) = U_n + U_{n+1}$. To fit into an $m \times m$ grid, z_n is such that $U_{n+1} \leq m$. We thus obtain that $n \leq \frac{\log(2\sqrt{2}m)}{\log(1+\sqrt{2})} - 1$. \square

We give now the upper and lower bounds for the number of maximal segments on finite CDP.

Theorem 3.15. *The number of maximal segments on a CDP enclosed into a $m \times m$ grid is bounded by:*

$$\frac{n_e(\Gamma)}{K_1 \log m + K_2} \leq n_{MS}(\Gamma) \leq 3n_e(\Gamma)$$

with $K_1 = \frac{2}{\log(1+\sqrt{2})}$ and $K_2 = \frac{\log 8(\sqrt{2}-1)}{\log(1+\sqrt{2})}$

Table 2: Constructions of $(R_i)_{1 \leq i \leq n}$ and $(L_i)_{1 \leq i \leq n}$ given n even.
 Constructions of $(R_i)_{1 \leq i \leq n}$ when $n = 2i$

Factor	Freeman moves	Depth
R_1	$E(z_{2i-1})^{u_{2i}-r_1}$	$2i - 1$
R_2	$E(z_{2i-2})^{u_{2i-1}-r_2} E(z_{2i-3})$	$2i - 1$
R_3	$E(z_{2i-3})^{u_{2i-2}-r_3}$	$2i - 3$
R_4	$E(z_{2i-4})^{u_{2i-3}-r_4} E(z_{2i-5})$	$2i - 3$
\vdots	\vdots	\vdots
R_{2j}	$E(z_{2i-2j})^{u_{2i+1-2j}-r_{2j}} E(z_{2i-1-2j})$	$2i + 1 - 2j$
R_{2j+1}	$E(z_{2i-1-2j})^{u_{2i-2j}-r_{2j+1}}$	$2i - 1 - 2j$
\vdots	\vdots	\vdots
R_{2i}	$0^{u_1-r_{2i}} 1$	1

Constructions of $(L_i)_{1 \leq i \leq n}$ when $n = 2i$

Factor	Freeman moves	Depth
L_1	$E(z_{2i-2}) E(z_{2i-1})^{u_{2i}-l_1}$	$2i$
L_2	$E(z_{2i-2})^{u_{2i-1}-l_2}$	$2i - 2$
L_3	$E(z_{2i-4}) E(z_{2i-3})^{u_{2i-2}-l_3}$	$2i - 2$
L_4	$E(z_{2i-4})^{u_{2i-3}-l_4}$	$2i - 4$
\vdots	\vdots	\vdots
L_{2j}	$E(z_{2i-2j})^{u_{2i+1-2j}-l_{2j}}$	$2i - 2j$
L_{2j+1}	$E(z_{2i-2-2j}) E(z_{2i-1-2j})^{u_{2i-2j}-l_{2j+1}}$	$2i - 2j$
\vdots	\vdots	\vdots
L_{2i}	$0^{u_1-l_{2i}}$	0

Proof. We know that maximal segments cover the entire discrete curve and that a maximal segment of depth n contains at most $2n + 1$ digital edges. Thus there cannot be less maximal segments than $n_e(\Gamma)/(2n + 1)$. Preceding corollary yields:

$$n \leq \frac{\log(2\sqrt{2}m)}{\log(1 + \sqrt{2})} - 1$$

Which leads to the inequality:

$$\frac{n_e(\Gamma) \log(1 + \sqrt{2})}{2 \log m + \log 8(\sqrt{2} - 1)} \leq n_{MS}(\Gamma) \leq \frac{n_e(\Gamma)}{2n + 1}$$

Theorem 3.11 brings the upper bound, putting both inequalities together bring:

$$\frac{n_e(\Gamma)}{K_1 \log m + K_2} \leq n_{MS}(\Gamma) \leq 3n_e(\Gamma)$$

4 Length of maximal digital straight segments

We present in this part how the length of maximal segments and of digital edges are tightly intertwined. We call \mathcal{L}^1 the length estimator based on the Minkowski

distance. For a vector \mathbf{u} we write $\mathcal{L}^1(\mathbf{u})$ and for a 4-connected discrete path $[AB]$ we write $\mathcal{L}^1([AB])$. Note that if $[AB]$ is a DSS then $\mathcal{L}^1([AB]) = \mathcal{L}^1(\mathbf{AB})$.

We begin our study by comparing the length of edge-supported with the length of its associated supporting edge (Proposition 4.1). We similarly study vertex-supported segments (Proposition 4.2).

Proposition 4.1. *Let $[V_k V_{k+1}]$ be a supporting edge of slope $\frac{a}{b}$ made of f patterns (a, b) and let MS be the maximal segment associated with it (Lemma 3.5). Their lengths are linked by the inequalities:*

$$\mathcal{L}^1(V_k V_{k+1}) \leq \mathcal{L}^1(MS) \leq \frac{f+2}{f} \mathcal{L}^1(V_k V_{k+1}) - 2$$

$$\frac{1}{3} \mathcal{L}^1(MS) < \mathcal{L}^1(V_k V_{k+1}) \leq \mathcal{L}^1(MS) < 3 \mathcal{L}^1(V_k V_{k+1})$$

Proof. Vertices V_k and V_{k+1} are leftmost and rightmost upper leaning points of MS . The points $V_k - (b, a)$, $V_{k+1} + (b, a)$ while clearly upper leaning points of the standard line going through $[V_k V_{k+1}]$ cannot belong to the CDP. Hence MS cannot extend further of its supporting edge of more than $|a| + |b| - 1$ points on both sides. Consequently $\mathcal{L}^1(MS) \leq \mathcal{L}^1(V_k V_{k+1}) + 2(|a| + |b| - 1)$. Using $\mathcal{L}^1(V_k V_{k+1}) = f(|a| + |b|)$ brings: $\mathcal{L}^1(V_k V_{k+1}) \leq \mathcal{L}^1(MS) \leq \frac{f+2}{f} \mathcal{L}^1(V_k V_{k+1}) - 2$. Worst cases bring $\mathcal{L}^1(V_k V_{k+1}) \leq \mathcal{L}^1(MS) < 3 \mathcal{L}^1(V_k V_{k+1})$ \square

Proposition 4.2. *Let MS be a vertex-supported segment and V_k its upper leaning point which is a vertex of the CDP. The length of this maximal segment is upper bounded by:*

$$\mathcal{L}^1(MS) \leq 4(\mathcal{L}^1(V_{k-1} V_k) + \mathcal{L}^1(V_k V_{k+1}))$$

Proof. We call L_1 , L_2 the leftmost and rightmost lower leaning points and $U_2 \equiv V_k$ the upper leaning point (see Fig. 3). Suppose that MS has a slope with an odd depth (say $2i + 1$).

Proposition B.1 implies $\mathcal{L}^1(\mathbf{L}_1 \mathbf{U}_2) = q_{2i} + p_{2i}$. There is clearly a right part of $[L_1 U_2]$ (i.e. $[L_1 V_k]$) that is contained in $[V_{k-1} V_k]$ and touches V_k . The pattern $E(z_{2i-1})^{u_{2i}}$ is a right factor of $[L_1 U_2]$ (Proposition B.1 again). It is indeed a right factor of $[V_{k-1} V_k]$ too, since it cannot extend further than V_{k-1} to the left without defining a longer digital edge. We get $[V_{k-1} V_k] \supseteq E(z_{2i-1})^{u_{2i}}$ and immediately $\mathcal{L}^1(V_{k-1} V_k) \geq u_{2i} \mathcal{L}^1(E(z_{2i-1})) = u_{2i}(q_{2i-1} + p_{2i-1})$.

From Eq. (2) and Eq. (3), we have: $q_{2i} + p_{2i} = u_{2i}(q_{2i-1} + p_{2i-1}) + q_{2i-2} + p_{2i-2}$ and $q_{2i-2} + p_{2i-2} \leq q_{2i-1} + p_{2i-1}$. We obtain immediately $\mathcal{L}^1(\mathbf{L}_1 \mathbf{U}_2) = q_{2i} + p_{2i} \leq (u_{2i} + 1)(q_{2i-1} + p_{2i-1})$. By comparing this length to the length of the digital edge $[V_{k-1} V_k]$, we get:

$$\mathcal{L}^1(\mathbf{L}_1 \mathbf{U}_2) \leq \frac{u_{2i} + 1}{u_{2i}} \mathcal{L}^1(V_{k-1} V_k)$$

Proposition B.1 and similar arguments on $[V_k V_{k+1}]$ bring :

$$\mathcal{L}^1(\mathbf{U}_2 \mathbf{L}_2) \leq \frac{u_{2i+1}}{u_{2i+1} - 1} \mathcal{L}^1(V_{k-1} V_k)$$

Worst cases are then $\mathcal{L}^1(\mathbf{L}_1 \mathbf{U}_2) \leq 2 \mathcal{L}^1(V_{k-1} V_k)$ and $\mathcal{L}^1(\mathbf{U}_2 \mathbf{L}_2) \leq 2 \mathcal{L}^1(V_k V_{k+1})$. The case where MS has a slope with an even depth (say $2i$) uses Proposition B.2

and for the same reasons as above leads to:

$$\mathcal{L}^1(\mathbf{L}_1 \mathbf{U}_2) \leq \frac{u_{2i}}{u_{2i}-1} \mathcal{L}^1(V_{k-1} V_k) \leq 2\mathcal{L}^1(V_{k-1} V_k)$$

$$\mathcal{L}^1(\mathbf{U}_2 \mathbf{L}_2) \leq \frac{u_{2i-1}+1}{u_{2i-1}} \mathcal{L}^1(V_k V_{k+1}) \leq 2\mathcal{L}^1(V_k V_{k+1})$$

Since MS has only one upper leaning point, it cannot be extended further than $\mathcal{L}^1(\mathbf{U}_2 \mathbf{L}_2)$ on the left and $\mathcal{L}^1(\mathbf{L}_1 \mathbf{U}_2)$ on the right (Lemma 3.5). Thus, we get:

$$\mathcal{L}^1(MS) \leq 4(\mathcal{L}^1(V_{k-1} V_k) + \mathcal{L}^1(V_k V_{k+1})) \quad \square$$

We are now able to compare the total length of maximal segments with the perimeter of the DCP.

Proposition 4.3. *Let Γ be a CDP, $n_{MS}(\Gamma)$ the number of maximal segment on Γ , then :*

$$\sum_{i \in n_{MS}(\Gamma)} \mathcal{L}^1(MS_i) \leq 19Per(\Gamma)$$

Proof. *With the notations of Theorem 3.11 and with slight abuse of notations, we decompose the total length as:*

$$\sum_{n_{MS}} \mathcal{L}^1(MS_i) = \sum_{n_{ULU}} \mathcal{L}^1(MS_{ULU}) + \sum_{n_{LUL}^{odd}} \mathcal{L}^1(MS_{LUL}^{odd}) + \sum_{n_{LUL}^{even}} \mathcal{L}^1(MS_{LUL}^{even})$$

Let us now focus on $\sum_{n_{ULU}} \mathcal{L}^1(MS_{ULU})$, using Proposition 4.1 we get :

$$\sum_{n_{ULU}} \mathcal{L}^1(MS_{ULU}) \leq 3 \sum_{n_{ULU}} \mathcal{L}^1([V_k V_{k+1}])$$

Using $n_{ULU} \leq n_e(\Gamma)$ and the fact that each digital edge appears at most once lead us to $\sum_{n_{ULU}} \mathcal{L}^1([V_k V_{k+1}]) \leq Per(\Gamma)$ entailing that:

$$\sum_{n_{ULU}} \mathcal{L}^1(MS_{ULU}) \leq 3Per(\Gamma)$$

Considering $\sum_{n_{LUL}^{odd}} \mathcal{L}^1(MS_{LUL}^{odd})$ and $\sum_{n_{LUL}^{even}} \mathcal{L}^1(MS_{LUL}^{even})$ with Proposition 4.2 we have:

$$\sum_{n_{LUL}^{odd}} \mathcal{L}^1(MS_{LUL}^{odd}) \leq 4 \sum_{n_{LUL}^{odd}} (\mathcal{L}^1([V_{k-1} V_k]) + \mathcal{L}^1([V_k V_{k+1}]))$$

$$\sum_{n_{LUL}^{even}} \mathcal{L}^1(MS_{LUL}^{even}) \leq 4 \sum_{n_{LUL}^{even}} (\mathcal{L}^1([V_{k-1} V_k]) + \mathcal{L}^1([V_k V_{k+1}]))$$

Considering that $n_{LUL}^{odd} \leq n_e(\Gamma)$ (from Proposition 3.10) and $n_{LUL}^{even} \leq n_e(\Gamma)$ (from Proposition 3.9) and that each digital edge appears at most once, we clearly get :

$$\sum_{n_{LUL}^{odd}} \mathcal{L}^1(MS_{LUL}^{odd}) \leq 4 \left(\sum_{n_{LUL}^{odd}} \mathcal{L}^1([V_{k-1} V_k]) + \sum_{n_{LUL}^{odd}} \mathcal{L}^1([V_k V_{k+1}]) \right) \leq 8Per(\Gamma)$$

$$\sum_{n_{LUL}^{even}} \mathcal{L}^1(MS_{LUL}^{even}) \leq 4 \left(\sum_{n_{LUL}^{even}} \mathcal{L}^1([V_{k-1}V_k]) + \sum_{n_{LUL}^{even}} \mathcal{L}^1([V_kV_{k+1}]) \right) \leq 8Per(\Gamma)$$

Eventually putting everything together brings:

$$\sum_{n_{MS}} \mathcal{L}^1(MS_i) \leq 19Per(\Gamma) \quad \square$$

We are now able to bound the average length of maximal segments wrt the number of edges on a CDP and the grid in which it is enclosed.

Theorem 4.4. *Let Γ be a CDP enclosed in a $m \times m$ grid, we have :*

$$\frac{Per(\Gamma)}{3n_e(\Gamma)} \leq \frac{\sum_{n_{MS}} \mathcal{L}^1(MS_i)}{n_{MS}(\Gamma)} \leq \frac{19Per(\Gamma)(K_1 \log m + K_2)}{n_e(\Gamma)}$$

with K_1 and K_2 defined as in Theorem 3.15.

Proof. *From Theorem 3.15 we get :*

$$\frac{1}{3n_e(\Gamma)} \leq \frac{1}{n_{MS}(\Gamma)} \leq \frac{K_1 \log m + K_2}{n_e(\Gamma)}$$

And from Proposition 4.3:

$$\sum_{n_{MS}} \mathcal{L}^1(MS_i) \leq 19Per(\Gamma)$$

Since maximal segments cover the entire discrete curve we have:

$$Per(\Gamma) \leq \sum_{n_{MS}} \mathcal{L}^1(MS_i)$$

It is now easy to see that:

$$\frac{Per(\Gamma)}{3n_e(\Gamma)} \leq \frac{\sum_{n_{MS}} \mathcal{L}^1(MS_i)}{n_{MS}(\Gamma)} \leq \frac{19Per(\Gamma)(K_1 \log m + K_2)}{n_e(\Gamma)}$$

We have thus shown that, on convex digital polygons, the average size of maximal segments is essentially proportional to the average size of the digital edges. Maximal segments may be slightly longer than digital edges on average by a logarithmic factor of the size of the grid containing the digital shape.

5 Asymptotic convergence

We may now turn to a direct application of the previous results of the paper by studying the asymptotic properties of discrete geometric estimators on digitized shapes. We therefore consider a plane convex body S which is contained in the square $[0, 1] \times [0, 1]$ (w.l.o.g.). Furthermore, we assume that its boundary $\gamma = \partial S$ is \mathcal{C}^3 with everywhere strictly positive curvature. This assumption is not very restrictive since people are mostly interested in regular shapes. Furthermore, the results of this section remains valid if the shape can be divided into a *finite* number of convex and concave parts; each one is then treated separately. The digitization of S with step $1/m$ defines a digital convex polygon $\Gamma(m)$ inscribed in a $m \times m$ grid. We first examine the asymptotic behavior of the maximal segments of $\Gamma(m)$, both theoretically and experimentally. We then study the *asymptotic convergence* of a discrete curvature estimator.

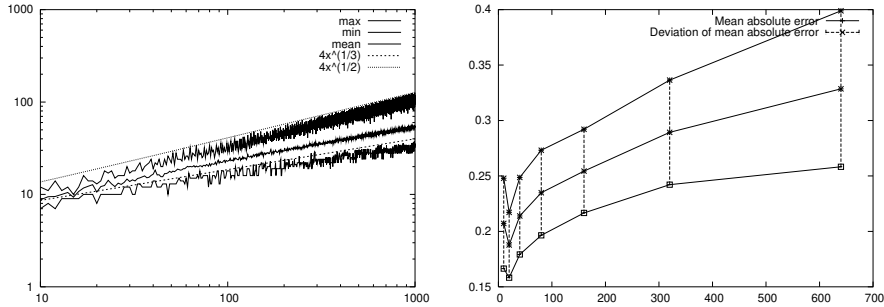


Figure 6: For both curves, the digitized shape is a disk of radius 1 and the abscissa is the digitization resolution. Left: plot in log-space of the \mathcal{L}^1 -size of maximal segments. Right: plot of the mean and standard deviation of the absolute error of curvature estimation, $|\hat{\kappa} - 1|$ (expected curvature is 1).

5.1 Asymptotic behavior of maximal segments

The next theorem summarizes the asymptotic average size of maximal segments with respect to the grid size m .

Theorem 5.1. *The average \mathcal{L}^1 -length $L(\Gamma(m))$ of the maximal segments of $\Gamma(m)$ has the following asymptotic bounds:*

$$\Theta(m^{\frac{1}{3}}) \leq L(\Gamma(m)) \leq \Theta(m^{\frac{1}{3}} \log m). \quad (7)$$

Proof. *Theorem 4.4 gives for the DCP $\Gamma(m)$ the following inequality:*

$$\frac{\text{Per}(\Gamma)}{3n_e(\Gamma)} \leq \frac{\sum_{n_{MS}} \mathcal{L}^1(MS_i)}{n_{MS}} \leq \frac{19\text{Per}(\Gamma)(K_1 \log m + K_2)}{n_e(\Gamma)}$$

where K_1 and K_2 are two constants.

Since $\Gamma(m)$ is convex and included in the subset $m \times m$ of the digital plane, its perimeter $\text{Per}(\Gamma(m))$ is upper bounded by $4m$. Furthermore, for a sufficiently large m , this perimeter is lower bounded by $p(\Gamma)m$, where $p(\Gamma)$ is twice the sum of the width and height of the bounding box of Γ . On the other hand, Theorem 2.7 indicates that its number of edges $n_e(\Gamma(m))$ is lower bounded by $c_1(S)m^{\frac{2}{3}}$ and upper bounded by $c_2(S)m^{\frac{2}{3}}$. Putting everything together gives:

$$\frac{p(\Gamma)m}{3c_2(\Gamma)m^{\frac{2}{3}}} \leq L(\Gamma(m)) \leq \frac{19 \times 4m \times (K_1 \log m + K_2)}{c_1(\Gamma)m^{\frac{2}{3}}}$$

which is once reduced what we wanted to show. \square

Although there are points on a shape boundary around which maximal segments grow as fast as $O(m^{\frac{1}{2}})$ (the critical points in [19]), most of them do not grow as fast.

On average, maximal segments grows as $\Theta(m^{\frac{1}{3}})$, this fact is confirmed with experiments. Fig. 6, left, plots the size of maximal segments for a disk digitized with increasing resolution.

5.2 Asymptotic convergence of discrete geometric estimators

A useful property that a discrete geometric estimator may have is to converge toward the geometric quantity of the continuous shape boundary when the digitization grid gets finer [4, 5, 17].

Of course, interesting discrete geometric estimator should converge for a large class of curves. We now recall the definition of a discrete curvature estimator based on DSS recognition [4].

Definition 5.2. *Let P be any point on a digital contour Γ in a grid of step $\frac{1}{m}$, $Q = B(P)$ and $R = F(P)$ are the extremities of the longest DSS starting from P (called half-tangents). Then the curvature estimator by circumcircle $\hat{\kappa}(P)$ is the inverse of the radius of the circle circumscribed to P , Q and R , rescaled by the resolution m .*

Experiments show that this estimator rather correctly estimates the curvature of discrete circles *on average* ($\approx 20\%$ error) at low resolution. It seems indeed better than any other curvature estimators proposed in the literature. Theorem B.4 of [4] demonstrates the *asymptotic convergence* of this curvature estimator, subject to the conjecture:

Conjecture 5.3. *Half-tangents on digitized boundaries grow at a rate of $\Theta(m^{\frac{1}{2}})$ with the resolution m .*

However, with our study of maximal segments, we can state that

Claim 5.4. *Conjecture 5.3 is not verified for digitizations of C^3 -curves with strictly positive curvature. We cannot conclude on the asymptotic convergence of the curvature estimator by circumcircle.*

Proof. *It is enough to note that half-tangents, being DSS, are included in maximal segments and may not be longer. Thus Theorem 5.1 concludes. \square*

The asymptotic convergence of a curvature estimator is thus still an open problem. Furthermore, precise experimental evaluation of this estimator indicates that it is most certainly not asymptotically convergent, although it is on average one of the most stable digital curvature estimator (see Fig. 6, right). Former experimental evaluations of this estimator were averaging the curvature estimates on all contour points. The convergence of the average of all curvatures does not induce the convergence of the curvature at one point.

6 Conclusion

As a conclusion, we have studied digital straight segments lying on convex digital shapes. We have shown several results relating quantities over maximal segments to the same quantities over digital edges. For shapes digitized at increasing resolutions, their asymptotic behaviour has also been studied. Contrary to what was thought before in the literature, maximal segments are shown to grow essentially at a rate of $m^{\frac{1}{3}}$ on average. These results will enable us in the future to find convergence rates for digital tangent estimators as well as defining a convergent digital curvature estimator.

A Digitization and 4 connected curves

Lemma A.1. *Let S be a convex subset of \mathbb{R}^2 then $\mathcal{D}(S) = \mathcal{D}(\text{conv}(\mathcal{D}(S)))$*

Proof. *First we prove that $\mathcal{D}(S)$ is always a subset of $\mathcal{D}(\text{conv}(\mathcal{D}(S)))$:*

$$\begin{aligned}\mathcal{D}(S) &\subseteq \text{conv}(\mathcal{D}(S)) \\ \mathcal{D}(\mathcal{D}(S)) &\subseteq \mathcal{D}(\text{conv}(\mathcal{D}(S))) \\ \mathcal{D}(S) &\subseteq \mathcal{D}(\text{conv}(\mathcal{D}(S)))\end{aligned}$$

We now prove that each element of $\mathcal{D}(\text{conv}(\mathcal{D}(S)))$ is in $\mathcal{D}(S)$. Let $x \in \mathcal{D}(\text{conv}(\mathcal{D}(S)))$, then $x \in \text{conv}(\mathcal{D}(S))$. Thus $x = \sum_i \lambda_i p_i$ with $\sum_i \lambda_i = 1$ and $\lambda_i \geq 0$ for all i . As for all i , $p_i \in \mathcal{D}(S)$, $p_i \in S$. Since S is a convex shape, $x \in S$. As $x \in \mathbb{Z}^2$, $x \in \mathcal{D}(S)$. \square

Lemma A.2. *For a given S where S is a plane convex body with \mathcal{C}^3 boundary and positive curvature, there exists m_S such that for all $m \geq m_S$, $\mathcal{D}_m(S)$ is connected.*

Proof. *There exists r_0 such that S is $\text{par}(r_0)$ -regular. Thus let $\mathcal{D}_m(S)$ with $m \geq \frac{2}{r_0}$. This entails that $m \cdot S$ is at least $\text{par}(2)$ -regular.*

Let us now suppose that for resolutions m larger than $\frac{2}{r_0}$, $\mathcal{D}_m(S)$ may have several connected components. Let C_1, C_2 be two connected component of $\mathcal{D}_m(S)$ and let p_1, p_2 be digital points in each component, C_1 and C_2 respectively.

Considering the complement of $\mathcal{D}_m(S)$ in \mathbb{Z}^2 there exists points outside $\mathcal{D}_m(S)$. We pick a point p'_1 such that we can build a 4-connected path \sqsubseteq_∞ from p_1 to p'_1 whom only point outside C_1 is p'_1 . \sqsubseteq_∞ is such that it is ordered and each element has a successor and a predecessor excepted the first and last elements. Moreover this path is chosen such that there exists a point of the boundary of $m \cdot S$ whom inside osculating ball (of radius mr_0) contains one point of \sqsubseteq_∞ which is not p'_1 . The same reasoning for C_2 leads to the 4-connected path \sqsubseteq_∞ and the point p'_2 .

As p'_1 and p'_2 are both on the boundary of $m \cdot S$, there exists a continuous path on the boundary of $m \cdot S$ from p'_1 to p'_2 . Let \mathcal{V} be the union of the inside osculating ball of radius mr_0 for each point of this continuous path. Since each ball has a radius larger than 2, the Gauss digitization of \mathcal{V} is 4-connected and inside the Gauss digitization of $m \cdot S$. This entails that there exists a 4-connected digital path between p_1 and p_2 . As a result, $\mathcal{D}_m(S)$ has only one connected component for resolution larger than a threshold depending on the $\text{par}(r)$ regularity of S . \square

Remark The two preceding lemmas entail that for large resolution, the Gauss digitization of convex shape with \mathcal{C}^3 boundary and positive curvature are always well-composed in the sense of [12, 21].

B Preliminary relations involving patterns

This section presents several properties related to patterns of DSS. They are used all along the paper. We may now compute vector relations between leaning points (upper and lower) inside a pattern. In the following we consider a DSS $(a, b, 0)$ in the first octant starting at the origin and ending at its second lower leaning point (whose coordinate along the x -axis is positive). We define $a/b =$

$z_n = [0, u_1, \dots, u_n]$ for some n . Leaning points will be called U_1, L_1, U_2 and L_2 as shown in Fig. 3. By definition $\mathbf{U}_1\mathbf{U}_2 = \mathbf{L}_1\mathbf{L}_2 = (b, a)$ and $\mathbf{U}_1\mathbf{L}_1 = \mathbf{U}_2\mathbf{L}_2$. We recall that the Freeman moves of $[U_1L_1]$ are the same as those of $[U_2L_2]$. Furthermore Freeman moves between U_1 and U_2 form the *pattern* (a, b) and those between L_1 and L_2 form the *reversed pattern* (a, b) . Proposition B.1 and Proposition B.2 indicate more precisely where leaning points lie within a pattern.

Proposition B.1. *A pattern with an odd depth (say $n = 2i + 1$) is such that $\mathbf{U}_1\mathbf{L}_1 = (u_{2i+1} - 1)(q_{2i}, p_{2i}) + (q_{2i-1}, p_{2i-1}) + (1, -1)$ and $\mathbf{L}_1\mathbf{U}_2 = (q_{2i} - 1, p_{2i} + 1)$. Moreover the DSS $[U_1L_1]$ has $E(z_{2i})^{u_{2i+1}-1}$ as a left factor, and the DSS $[L_1U_2]$ has $E(z_{2i-1})^{u_{2i}}$ as a right factor.*

Proof. From Eq. (1) we have: $p_{2i+1}q_{2i} - p_{2i}q_{2i+1} = (-1)^{2i+1+1} = 1$, which can be rewritten as: $aq_{2i} - bp_{2i} = 1$. Thus q_{2i} and p_{2i} are clearly the Bézout coefficients of (a, b) . One can check that point $(b + 1 - q_{2i}, a - 1 - p_{2i})$ is L_1 : its remainder is $a + b - 1$ and its x -coordinate while positive is smaller than b . We immediately get $\mathbf{U}_1\mathbf{L}_1 = (b + 1 - q_{2i}, a - 1 - p_{2i})$.

Using Eq. (3) yields: $\mathbf{U}_1\mathbf{L}_1 = ((u_{2i+1} - 1)q_{2i} + q_{2i-1} + 1, (u_{2i+1} - 1)p_{2i} + p_{2i-1} - 1)$. From $\mathbf{L}_1\mathbf{U}_2 = -\mathbf{U}_1\mathbf{L}_1 + \mathbf{U}_1\mathbf{U}_2$, we further get that $\mathbf{L}_1\mathbf{U}_2 = (q_{2i} - 1, p_{2i} + 1)$. From Eq. (5) $E(z_{2i})^{u_{2i+1}-1}$ is a left factor of $[U_1U_2]$ but also of $[U_1L_1]$. Writing $E(z_{2i+1})$ as $E(z_{2i})^{u_{2i+1}-1}E(z_{2i-2})E(z_{2i-1})^{u_{2i+1}}$, and expanding $\mathbf{L}_1\mathbf{U}_2$ as $(u_{2i}q_{2i-1} + q_{2i-2} - 1, u_{2i}p_{2i-1} + p_{2i-2} + 1)$ with Eq. (2), we see that $E(z_{2i-1})^{u_{2i}}$ is a right factor of $[L_1U_2]$. \square

Proposition B.2. *A pattern with an even depth (say $n = 2i$) is such that $\mathbf{U}_1\mathbf{L}_1 = (q_{2i-1} + 1, p_{2i-1} - 1)$ and $\mathbf{L}_1\mathbf{U}_2 = (u_{2i} - 1)(q_{2i-1}, p_{2i-1}) + (q_{2i-2}, p_{2i-2}) + (-1, 1)$. Moreover the DSS $[U_1L_1]$ has $E(z_{2i-2})^{u_{2i}-1}$ as a left factor, and the DSS $[L_1U_2]$ has $E(z_{2i-1})^{u_{2i}-1}$ as a right factor.*

The proof is similar to the proof of Proposition B.1 and may be found in [9]. Patterns and sub-patterns that are right or left factors have their slopes closely related, as shown by Proposition B.3 and Proposition B.4.

Proposition B.3. *If the odd pattern $E(z'_{2p+1})$ with $z'_{2p+1} = [0, u'_1, \dots, u'_{2p+1}]$ is a right factor of the pattern $E(z_k)$ with $z_k = [0, u_1, \dots, u_k]$ then:*

$$z'_{2p} = z_{2p} \quad \text{and} \quad u'_{2p+1} \leq u_{2p+1}$$

Proof. Consider two patterns $E(z_k)$ and $E(z'_{2p+1})$ with $z_k = [0, u_1, \dots, u_k]$ and $z'_{2p+1} = [0, u'_1, \dots, u'_{2p+1}]$. From Eq (5) and (6) it is clear that $E(z_k)$ always ends with an odd pattern whatever k . Consider there exists i ($2i + 1 \leq k$) such that $E(z_{2i-1}) \subseteq E(z'_{2p+1}) \subseteq E(z_{2i+1})$ as shown on Fig. 7. If $E(z'_{2p+1})$ equals $E(z_{2i+1})$ then from unicity of decomposition in simple continued fraction we get $p = i$ and $z'_{2p+1} = z_{2p+1}$. Which concludes this case. Otherwise looking at the decomposition of $E(z_{2i+1})$ from Eq (5) and (6), there exists j , with $0 \leq j < u_{2i+1}$ such that $E(z_{2i})^j E(z_{2i-1}) \subseteq E(z'_{2p+1}) \subsetneq E(z_{2i})^{j+1} E(z_{2i-1})$, whose slopes are $[0, u_1, \dots, u_{2i}, j]$ and $[0, u_1, \dots, u_{2i}, j + 1]$. Any discrete path P such that $E(z_{2i})^j E(z_{2i-1}) \subseteq P \subsetneq E(z_{2i})^{j+1} E(z_{2i-1})$ analyzed by the standard DSS recognition algorithm [8] is recognized as a DSS with a slope equal to $[0, u_1, \dots, u_{2i}, j]$. Thus the slope of $E(z'_{2p+1})$ is also $[0, u_1, \dots, u_{2i}, j]$. More precisely, being a pattern, $E(z'_{2p+1}) = E([0, u_1, \dots, u_{2i}, j])$, this entails $z'_{2p+1} = [0, u_1, \dots, u_{2i}, j]$ and $p = i$.

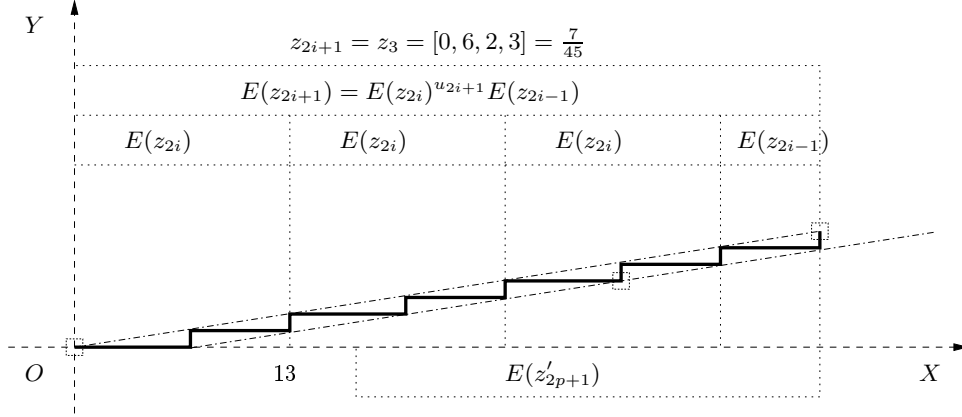


Figure 7: The odd pattern $E(z_{2i-1}) \subseteq E(z'_{2p+1}) \subsetneq E(z_{2i+1})$

Consider now that there is no i such that: $E(z_{2i-1}) \subseteq E(z'_{2p+1}) \subseteq E(z_{2i+1})$. This means that we cannot find two odd sub-patterns belonging to $E(z_k)$ bounding $E(z'_{2p+1})$. As a result we have: $E(z_{k-1}) \subseteq E(z'_{2p+1}) \subseteq E(z_k)$ with k being even, we have $E(z_k) = E(z_{k-2})E(z_{k-1})^{u_k}$ and we may consider two cases:

- there exist j such that $E(z_{k-1})^j \subseteq E(z'_{2p+1}) \subseteq E(z_{k-1})^{j+1}$, with $j+1 \leq u_k$,
- or $E(z_{k-1})^{u_k} \subsetneq E(z'_{2p+1}) \subseteq E(z_k)$

In the first case, it is clear that $E(z'_{2p+1})$ is recognized by the standard DSS recognition algorithm as a DSS of slope z_{k-1} since it is bounded by two discrete paths of slope z_{k-1} . In this case we get $z_{k-1} = z'_{2p+1}$.

In the other case, let us note that $E(z_{k-1}) \subset E(z'_{2p+1})$, which implies that $E(z_{k-1})$ is bounded by two odd sub-patterns of $E(z'_{2p+1})$. Thus using the same reasoning as earlier-on we get $z'_{k-2} = z_{k-2}$ and $u_{k-1} \leq u'_{k-1}$. From Eq (5) and (6), it is clear that every pattern begins with even pattern whatever their depth. As a result $E(z_{k-2})$ is a left factor of $E(z'_{2p+1})$ and $E(z_k)$. Moreover since $E(z_{k-1})^{u_k} \subsetneq E(z'_{2p+1}) \subseteq E(z_k) \equiv E(z_{k-2})E(z_{k-1})^{u_k}$, $E(z'_{2p+1})$ and $E(z_k)$ begin with the same even pattern. Consequently $E(z_k)$ must be equal to $E(z'_{2p+1})$. Since those patterns do not have the same parity of depth it raises a contradiction and this case cannot happen. This concludes the proof. \square

Proposition B.4. If the even pattern $E(z'_{2p})$ with $z'_{2p} = [0, u'_1, \dots, u'_{2p}]$ is a left factor of the pattern $E(z_k)$ with $z_k = [0, u_1, \dots, u_k]$. We have:

$$z'_{2p-1} = z_{2p-1} \quad \text{and} \quad u'_{2p} \leq u_{2p}$$

Proof. see [9]. \square

References

- [1] A. Balog and I. Bárány. On the convex hull of the integer points in a disc. In *SCG '91: Proceedings of the seventh annual symposium on Computational geometry*, pages 162–165. ACM Press, 1991.

- [2] I. Barany and D. G. Larman. The convex hull of the integer points in a large ball. *Math. Annalen*, 312:167–181, 1998.
- [3] J. Berstel and A. De Luca. Sturmian words, lyndon words and trees. *Theoret. Comput. Sci.*, 178(1-2):171–203, 1997.
- [4] D. Coeurjolly. *Algorithmique et géométrie pour la caractérisation des courbes et des surfaces*. PhD thesis, Université Lyon 2, Décembre 2002.
- [5] D. Coeurjolly and R. Klette. A comparative evaluation of length estimators of digital curves. *IEEE Trans. on Pattern Anal. and Machine Intell.*, 26(2):252–257, 2004.
- [6] D. Coeurjolly, S. Miguët, and L. Tougne. Discrete curvature based on osculating circle estimation. In C. Arcelli, L.P. Cordella, and G. Sanniti di Baja, editors, *Proc. 4th Int. Workshop on Visual Form (IWVF4)*, LNCS 2059, pages 303–312. Springer-Verlag, Berlin, 2001.
- [7] F. de Vieilleville, J.-O. Lachaud, and F. Feschet. Maximal digital straight segments and convergence of discrete geometric estimators. In H. Kalviainen, J. Parkkinen, and A. Kaarna, editors, *14th Scandinavian Conference on Image Analysis*, LNCS 3540, pages 988–997. Springer-Verlag, 2005.
- [8] I. Debled and J.-P. Réveillès. A linear algorithm for segmentation of digital curves. *IJPRAI*, 9(4):635–662, 1995.
- [9] J.-O. Lachaud F. de Vieilleville and F. Feschet. Maximal digital straight segments and convergence of discrete geometric estimators. Research Report 1350-05, LaBRI, University Bordeaux 1, Talence, France, 2005.
- [10] F. Feschet and L. Tougne. Optimal time computation of the tangent of a discrete curve: application to the curvature. In *Discrete Geometry and Computer Imagery (DGCI)*, LNCS 1568, pages 31–40. Springer Verlag, 1999.
- [11] F. Feschet and L. Tougne. On the min dss problem of closed discrete curves. *Discrete Applied Math.*, 151(1-3):138–153, 2005.
- [12] A. Gross and L. Latecki. Digitizations preserving topological and differential geometric properties. *Comput. Vis. Image Underst.*, 62(3):370–381, 1995.
- [13] G. H. Hardy and E. M. Wright. *An introduction to the theory of numbers*. Oxford University Press, fourth edition, 1960.
- [14] A. S. Hayes and D. C. Larman. The vertices of the knapsack polytope. *Discrete Applied Mathematics*, 6:135–138, 1983.
- [15] C. E. Kim. Digital convexity, straightness, and convex polygons. *IEEE Trans. on Pattern Anal. and Machine Intell.*, 6(6):618–626, 1982.
- [16] R. Klette and A. Rosenfeld. *Digital Geometry - Geometric Methods for Digital Picture Analysis*. Morgan Kaufmann, San Francisco, 2004.

- [17] R. Klette and J. Žunić. Multigrid convergence of calculated features in image analysis. *Journal of Mathematical Imaging and Vision*, 13:173–191, 2000.
- [18] V. Kovalevsky and S. Fuchs. Theoretical and experimental analysis of the accuracy of perimeter estimates. In Förster and Ruwiedel, editors, *Proc. Robust Computer Vision*, pages 218–242, 1992.
- [19] J.-O. Lachaud. On the convergence of some local geometric estimators on digitized curves. Research Report 1347-05, LaBRI, University Bordeaux 1, Talence, France, 2005.
- [20] J.-O. Lachaud, A. Vialard, and F. de Vieilleville. Analysis and comparative evaluation of discrete tangent estimators. In E. Andrès, G. Damiand, and P. Lienhardt, editors, *Proc. Int. Conf. Discrete Geometry for Computer Imagery*, LNCS 3429, pages 240–251. Springer-Verlag, 2005.
- [21] L. J. Latecki, C. Conrad, and A. Gross. Preserving topology by a digitization process. *Journal of Mathematical Imaging and Vision*, 8(2):131–159, mar 1998.
- [22] H. Reiter-Doerksen and I. Debled-Rennesson. Convex and concave parts of digital curves. In *Dagstuhl Seminar "Geometric Properties from Incomplete Data"*, March 2004.
- [23] J.-P. Réveillès. *Géométrie discrète, calcul en nombres entiers et algorithmique*. Thèse d'état, Université Louis Pasteur, Strasbourg, 1991. In french.
- [24] V. N. Shevchenko. On the number of extreme points in linear programming. *Kibernetika*, 2:133–134, 1981. In russian.
- [25] K. Voss. *Discrete Images, Objects, and Functions in \mathbb{Z}^n* . Springer-Verlag, 1993.